Diatoms as a paleoproductivity proxy in the NW Iberian coastal upwelling system (NE Atlantic)

Diana Zúñiga[1,2], Celia Santos[3,4], María Froján[2], Emilia Salgueiro[3,5], Marta M. Rufino[3,5], Francisco De la Granda[6]. Francisco G. Figueiras[2], Carmen G. Castro[2], Fátima Abrantes[3,5]

[1] University of Vigo, Applied Physics Department, Campus Lagoas Marcosende, E-36310, Vigo, Spain
[2] Consejo Superior de Investigaciones Científicas (CSIC), Instituto de Investigaciones Marinas (IIM), E-36208, Vigo, Spain
[3] Instituto Português do Mar e da Atmosfera (IPMA), Div. Geologia e Georecursos Marinhos, 1495-006, Lisbon, Portugal
[4] MARUM, Center for Marine Environmental Sciences, University of Bremen, 28359, Bremen, Germany.
[5] CCMAR - Centre of Marine Sciences. Universidade do Algarve, Campus de Gambelas, 8005-139 Faro
[6] Bundesamt für Seeschifffahrt und Hydrographie, Bernhard-Nocht-Str. 78, 20359, Hamburg, Germany

Correspondence to: Diana Zúñiga (diana.zuniga@uvigo.es; imissons@gmail.com)

Abstract. The objective of the current work is to improve our understanding as to how diatoms species determine primary production signal in exported and buried particles. We evaluated how the diatom's abundance and assemblage composition is transferred from the photic zone to seafloor sediments. To address this, we used a combined analysis of water column, sediment trap and surface sediment samples recovered in the NW Iberian coastal upwelling system was used.

Diatom fluxes (2.2 ± 5.6 10^6 valves m^{-2} d^{-1}) represented the majority of the siliceous microorganisms sinking out from the photic zone during all studied years and showed strong seasonal variability. Discrepancies between water column-sediment trap diatom abundances were found, as shown by the unexpectedly high diatom export signals registered during low productive downwelling periods. They were principally related to surface sediment remobilization and intense Minho and Douro riverine discharges that constitute an additional source of particulate material to the inner continental shelf. Contributions of allochthonous particles to the sinking material were confirmed by the significant increase of both benthic and freshwater diatoms in the sediment trap assemblage.

Nevertheless, during highly productive upwelling periods no water column-sediment trap direct correlations were found in terms of absolute numbers. However, diatom species sinking out from the photic zone (principally represented by *Chaetoceros* and *Leptocylindru*s spp. resting spores) agreed with those species dominating the water column. This demonstrates that the prevalence of these highly resistant resting spores in the sediments reflect the dominance of both diatom taxa in the surface photic layer when primary production is seasonally intensified. Moreover, our data shows that *Chaetoceros* spp. resting spores dominated the sediment trap assemblage under persistent upwelling winds, high irradiance levels and cold and nutrient-rich waters, while *Leptocylindrus* spp. spore fluxes were favoured when northerly winds relaxed, and surface water warming promoted water column stratification. Further, this finding will enable the use of relative abundance of both groups in the sediment records as a proxy of persistent vs. intermittent upwelling conditions, which is of particular relevance to infer climatic and oceanographic conditions in the past.

Keywords: diatoms; coastal upwelling; organic carbon; biogenic silica; sediment trap; NW Iberian;

1 Introduction

The ocean plays a critical role in the global carbon cycle as a vast reservoir that takes up a substantial portion of the anthropogenically-released carbon from the atmosphere (LeQuéré et al., 2009). A key aspect to understand the ocean carbon cycle includes the role of diatoms as sinkers of primary-produced organic carbon and biogenic silica from the surface productive layer to the sediment record (Sancetta, 1989; Smetacek, 1999; Boyd and Trull, 2007; Romero and Armand, 2010; Tréguer and De La Rocha, 2013). This point underpins the importance and effectiveness of diatom species as productivity indicator in Earth´s climate system studies.

Despite the significant advances in this topic, primary production paleoreconstructions via diatom species still require regional calibrations to better understand their response to particular environmental conditions, and to analyse which species transfer the primary production signal via exported and buried particles. Coastal upwelling systems, as sites of major primary production with a marked seasonality are thus ideal for these types of studies (Walsh, 1991; Falkowski et al., 1998; Capone and Hutchins, 2013). The importance and the effectiveness of diatoms as productivity indicators at longer time scales in highly productive coastal regions have been shown by many long-term continuous datasets (Sancetta, 1995; Lange et al., 1998; Romero et al., 2002; Abrantes et al., 2002; Venrick et al., 2003; Onodera et al., 2005).

In the NW Iberian margin where seasonal upwelling favouring winds generate high primary production rates through modulation of the microplankton community structure (Figueiras and Pazos, 1991; Nogueira and Figueiras, 2005; Espinoza-González et al., 2012), several works have assessed the diatom species ecology – in terms of its environmental conditions by comparing the recent sediment record to the hydrographic conditions (Abrantes, 1988; Bao et al., 1997; Abrantes and Moita, 1999; Gil et al., 2007; Bernárdez et al., 2008; Abrantes et al., 2011). Those authors concluded that the spatial distribution of the sedimentary diatom abundance and assemblages´ composition reflects the hydrographic upwelling patterns and primary production trends, with *Chaetoceros* resting spores appearing as a good tracer of the upwelling regime.

The aim of this study is to understand the seasonal mechanisms regulating diatom production and export from the photic zone into the seafloor sediments in the NW Iberian coastal upwelling system, through the combined analysis of diatom abundances and assemblages composition in the water column, sediment trap and surface sediment samples.

2 Regional setting

Our study site (RAIA station) is located in the NW Iberian continental shelf off Cape Silleiro (42º 05´ N; 8º 56´ W at 75 m water depth, Fig. 1). During spring – summer, the NW Iberian coast is characterized by prevailing northerly winds, that favour upwelling of cold and nutrients rich subsurface Eastern North Atlantic Central Water (ENACW) on the shelf and into the Rías, resulting in a primary production increase in the area (Fraga, 1981; Fiuza, 1984; Tenore et al., 1995: Figueiras et al., 2002). In contrast, south-westerly winds favour coastal downwelling during autumn-winter. Hydrographically, from

October to January the region is generally affected by the northward advection of warm, saline and nutrient-poor waters by the Iberian Poleward Current (IPC) (Haynes and Barton, 1990, Relvas et al., 2007). Later on, usually between February–March, a decrease of temperature associated with winter cooling leads to a well homogenized mixed layer of cold and nutrient rich waters (Álvarez–Salgado et al., 2003; Castro et al., 2006). In addition, during downwelling seasons, the occurrence of south-westerly winds can generate moderate to extreme storms with wave heights > 6 m, which have been simulated to produce high sediment remobilization (Vitorino et al., 2002; Jouanneau et a., 2002; Oberle et al., 2014). During these highly hydrodynamic periods, this region is also strongly influenced by the Minho and Douro Rivers discharge (annual averages of 550 $m^3 s^{-1}$ and 310 $m^3 s^{-1}$, respectively), which are important sources of terrestrial sediments to the inner shelf. This mainly occurs during the winter months, when river inflows can reach 3850 $m^3 s^{-1}$ for the Douro River and 1800 $m^3 s^{-1}$ for the Minho River (Dias et al., 2002; Otero et al., 2010)

3 Material and methods

3.1 External forcing

Irradiance data was obtained from Cies meteorological station (IR; 42° 13´ N, 8° 54´ W, 25 m height) (Fig. 1) and accessed via the MeteoGalicia website (www2.meteogalicia.es).

Daily Ekman transport ($-Q_x$), an estimate of the volume of upwelled water per kilometre of coast was calculated according to Bakun´s (1973) method:

$-Q_x = -((\rho_a CD |V|) / (f \rho_{sw})) V_y$

where ρ_a is the density of the air (1.22 kg m^{-3}) at 15 ºC, CD is an empirical dimensionless drag coefficient (1.4 10^{-3}), f is the Coriolis parameter (9.76 10^{-5}) at 42 ºN, ρ_{sw} is the seawater density (1025 kg m^{-3}) and |V| and V_y are the average daily module and northerly component of the geostrophic winds centred at 42º N, 10º W, respectively. Positive values show the predominance of northerly winds that induces upwelling on the shelf and negative values indicate the presence of downwelling. Minho and Douro River discharges were obtained from https://github.com/PabloOtero/uptodate_rivers (Otero et al., 2010). Wave data were based on WANA hindcast reanalysis of 3027034 ($WANA_S$: off Silleiro: 42º 15'N; 9º W) and 1044067 ($WANA_G$: off A Guardia: 41º 45´N; 9º W) (Fig. 1), and supplied by Puertos del Estado.

3.2 Water column

RAIA station (75 m water depth) was visited monthly on board "R/V *Mytilus*" from March 2009 to June 2012 except during the period December 2009-June 2010. Characterization of the water column was conducted by i) CTD-SBE25 profiling and ii) collection of discrete water column samples using a rosette sampler with 10-LPVC Niskin bottles for inorganic nutrients and chlorophyll *a* (Chl *a*) analysis, and diatoms counting and species identification.

Water column stability (0-35 m) was analysed by using Brunt Väisälä frequency parameter, $N^2 = [g / z] \ln (p_z/p_0)$ where g is the local acceleration of gravity, z is the water depth and p_z and p_0 the bottom and surface density, respectively.

Nutrients concentration was determined by segmented flow analysis with Alpkem autoanalysers (Hansen and Grasshoff, 1983). The analytical errors were ± 0.05 µmol kg^{-1} for nitrate and silicate, and ± 0.01 µmol kg^{-1} for phosphate. Final Chl *a* concentrations were determined by pigment extract fluorescence using a Turner Designs fluorometer calibrated with pure Chl *a* (Sigma) (see details in Zúñiga et al., 2016).

For diatoms counting and identification a volume of 100 ml sample from 5 water depth was used, taking into account that for the whole sampling period maximum variability of Chl *a* content occurred at the surface (Zúñiga et al., 2016). The samples were preserved with Lugol´s iodine until micrococoscopic observation. Depending on the water column Chl *a* concentration volumes varied between 10 to 50 mL and were deposited in composite sedimentation chambers for observation through an inverted microscope. The microorganisms were counted and identified to the species level, whenever possible, using the Utermöhl sedimentation method (Utermöhl, 1931, 1958). Centric diatom cells whose diameter did not allow for species identification were grouped as small centric diatoms. Only diatom species that appeared in more than one sample with a percentage higher than 2 % of the total abundance were considered for further analysis.

3.3 Sediment trap

At RAIA station an automated cylindric-conical Technicap PPS 4/3 sediment trap (height/diameter ratio of 1.7 and a collecting area of 0.05 m^2) was deployed at 35 m water depth from March 2009 to June 2012. Sampling intervals ranged from 4 to 12 days. Unfortunately some data were lost due to technical problems and bad weather conditions (Zúñiga et al., 2016). Examination of CTD pressure data mounted 2 m below the trap showed that the mooring line tilting was less than 5º during 70 % of the time it was deployed. In exceptional hydrodynamic events that lead to velocities higher than 25 cm s^{-1} the mooring tilted 15-20º. Therefore, we assume the trap was not affected by hydrodynamic biases. Sampling strategy and sample processing details are explained at length in Zúñiga et al. (2016).

Total mass flux was gravimetrically determined. Biogenic silica content was analysed following Mortlock and Froelich, (1989). The samples were treated with 2M Na_2CO_3 for 5 h at 85 ºC to extract the silica and then measure as dissolved silica by colorimetric reaction. Biogenic opal was converted from Si concentration after multiplying it by a factor of 2.4.

Sample preparation for diatom abundance and assemblage assessment was adapted from Abrantes et al. (2005). Depending on the recovered material 1/5 or 2/5 splits of the original samples were used, after rinsing with $HgCl_2$ by repeated settling in distilled water. Subsequently, organic matter and carbonates were removed by the addition of H_2O_2 (30 %) and HCl (10 %), respectively. Permanent slides were prepared using the evaporation-tray method of Battarbee, (1973) and Norland optical adhesive (NOA61) as the mounting medium. Diatoms counting and species identification was performed at 1000 X (10 x eyepieces and 100 x objectives), using a Nikon Eclipse E100 microscope equipped with Differential Interference Contrast

(DIC). 100 randomly selected fields of view were counted in 3 replicate slides (Abrantes et al., 2005). The diatom flux was calculated as follows:

F= ((N)(A/a) (V)(S)(X))/D

where the flux F is expressed as number of valves m^{-2} d^{-1}, N is the number of valves counted in 100 randomly selected fields of view, (a) represents the counted fraction of the total tray area (A), V is the dilution volume, S is the split fraction, X is the conversion factor from the collecting area to 1 m^2, and D is the sampling interval in days for each sample.

Relative abundance of diatom taxa was determined following the counting procedures from Schrader and Gersonde, (1978) and Abrantes, (1988). For each sample, ca. 300 individuals were identified to the lowest taxonomic possible level, and raw counts were converted to percentage abundance. In samples containing low diatom abundances, the number of individuals identified was 100 – 200 (Fatela and Taborda, 2002). For this study only diatom species that appeared in more than one sample with a percentage higher than 2% of the total abundance were considered for further analysis.

3.4 Surface sediments

To evaluate the sedimentary record, we used one core-top sediment (0 - 1 cm) from box-core GeoB 11002-1 (42º 10´N, 8º 58´ W; 111 m) recovered near the RAIA position (Fig. 1). The sample was collected in August 2006, using a giant box corer during the GALIOMAR expedition (P342) on board of the R/V *Poseidon*. Sample cleaning and slides preparation was carried out following the methodology of Abrantes et al. (2005). Counting and identification procedures were the same as for sediment traps samples.

3.5 Statistical data analysis

Relationships between environmental variables and between sediment trap diatom species relative abundances were evaluated with Pearson correlation coefficients and presented in Table 1 and 2, respectively.

In addition, the relationship between the relative abundance of the main groups of diatoms (freshwater diatoms, benthic diatoms, *Chaetoceros* resting spores, *Leptocylindrus* resting spores and *Paralia sulcata*) and the environmental variables were analysed using the ordination technique Canonical Correspondence Analysis (CCA) (vegan package, R-project (ter Braak, 1986; Oksanen et al., 2015). The water column environmental data was at first monthly interpolated and later averaged for the time interval recovered by each trap sample. Resulting data were subsequently integrated to 35 m where the sediment trap was moored. The multicollinearity of environmental variables was previously tested by Pearson correlations (Dormann et al., 2013) and checked after modelling using variance inflation factors (VIFs) applied to the CCA. Nine environmental variables were thus initially included in the ordination: irradiance, temperature, Brunt Väisälä frequency parameter (N^2), Chl *a*, NO_3, $Si(OH)_4$, upwelling index (UI), Minho River flow, A Guarda wave height (Hs). Significant environmental variables were identified via a stepwise procedure, using permutation tests (999 permutations). After the selection of the significant variables, the model was tested a second time through a Monte Carlo global permutation test (999 permutations) to assess the significance of ordination axes.

The results of CCA were presented as ordination bi-plot diagram containing the explanatory variables plotted as arrows along with points for samples (dates) and species (main groups of diatoms). Using these diagrams, we were able to identify the relationships between species, between samples, and relationships of samples and species to environmental variables.

4 Results

4.1 Environmental conditions and water column characteristics

From October to April-May, the NW Iberian margin was characterized by the prevalence of low irradiance levels and south-westerly winds as shown by the negative -Q_x values (Fig. 2a and 2b). During these periods the region was strongly affected by strong SW storms promoting wave heights frequently higher than 4 m, and intense Minho and Douro River discharges (Fig. 2c and 2d). As explained in detail in Zúñiga et al. (2016), hydrographically, we can distinguish in a first phase the presence of the IPC (October-January), characterized by anomalously warm water (15-17 ºC) with relatively low nutrient concentrations and Chl a (< 4 mg m^{-3}) (Fig. 3). Later on, we differentiate the mixing period (from February to April-May), with temperatures of around 14 ºC (due to winter cooling), and higher nutrient levels associated with intense river discharges (Fig. 2d, 3a, 3b and Table 1). During downwelling periods, diatom abundances were low (34 ± 49 cel mL^{-1}) with small centric diatoms accounting for the largest shares (52 ± 25 %). Only exceptionally *Navicula* spp. and *Paralia sulcata* become relevant (Fig. 3c, 4 and Table 3). On the other hand, from April- May to October, the margin was characterized by high irradiance levels and the upwelling of cold (< 14ºC) and nutrient rich ENACW on the continental shelf that leaded to the development of Chl *a* maxima (Fig. 3). During those highly productive upwelling periods, diatom abundances achieved maximum levels and the predominant genera in the water column alternated between *Chaetoceros* and *Leptocylindrus* spp. Other species frequently associated with upwelling favourable conditions (e.g. *Asterionellopsis glacialis*, *Detonula pumila* or *Guinardia delicatula*), appeared sporadically and with lower abundances (Fig. 4 and Table 3).

4.2 Sinking particulate material time series

The biogenic silica flux time series, as registered by the trap, contributes from 2% to 10% of the total material, and is closely follow by the siliceous organism fluxes calculated from microscopic counting (Fig. 5a, 5b and 5c). The contribution of diatoms to total siliceous microorganisms dominated throughout the entire period (Fig. 5c and 5e). Only during the 2012 upwelling season did silicoflagellates become relevant, achieving a relative abundance > 7 % (Fig. 5d). Maximum total diatom fluxes were registered under downwelling conditions (Fig. 5e). During these periods benthic and freshwater diatoms became relevant, contributing to the total diatom fluxes up of 24 % and 17 %, respectively (Fig. 6). On the contrary, during upwelling phases total diatom fluxes were relatively low, ranging around a mean seasonal value of 6 ± 10 10^5 valves m^{-2} d^{-1} (Fig. 5e and Table 3). During these periods, the diatom assemblage found in the trap samples were mainly composed of *Chaetoceros* spp. and *Leptocylindrus* spp. resting spores, with mean contributions to total marine diatom fluxes of 46 % and 20 %, respectively (Fig. 7 and Table 3).

4.3. Surface sediment samples

Diatom abundances in GeoB 11002-1 top sediment sample was 142 x 10^4 valves g^{-1}. Marine diatom assemblage was dominated by resting spores of both *Chaetoceros* (33%) and *Leptocylindrus* (37%) spp., and *Paralia sulcata* (17%) (Table 3). Benthic and freshwater diatoms had contributions < 4 %.

4.4 Relationships between sediment trap main diatom groups and environmental variables

Canonical correspondence analysis (CCA) stepwise procedure identified five significant variables for the abundance of the main diatom groups (p-value < 0.05), Minho River flow (Minho River), temperature (Temp), Chlorophyll *a* (Chl *a*), NO_3 and $Si(OH)_4$ (Fig. 8). The first two canonical axes explained 48.7 % and 40.4 %, i.e. 89 % of the modelled inertia and consequently only those two axes were considered. The CCA model with the five variables explained 46% of the total inertia. The first canonical axis showed a positive gradient with Temp and Chl *a* opposite to Minho River discharge. Freshwater (FW) diatoms, benthic diatoms and *Paralia sulcata* (Parsul) were negatively positioned in the first canonical axis, indicating thus a positive relationship with the Minho River, and a negative relationship with temperature and Chl *a*. The second canonical axis showed a negative gradient with NO_3 and $Si(OH)_4$ and a negative relationship between these variables and *Chaetoceros* resting spores (ChaeRS). Conversely, *Leptocylindrus* resting spores (LepRS) were positively related with NO_3 and $Si(OH)_4$. The temporal distribution of the sediment trap samples confirmed that FW diatoms, benthic diatoms and Parsul occurred mainly during downwelling months while ChaeRS and LepRS were associated to upwelling periods (Fig. 8). In addition, this figure also identifies LepRS with late summer and IPC periods.

5 Discussion

The siliceous microorganism fluxes determined from the sediment trap, mostly represented by diatoms, showed significant discrepancies with water column diatom abundances (Fig. 3c, 5c and 5e). Such discrepancies were determined by the NW Iberian inner continental margin hydrodynamics, as explained in detail by Zúñiga et al. (2016). These authors described how maximum particle fluxes occurring during downwelling periods were associated with allochthonous sources, explaining the a priori contradictory observation of maximum diatom fluxes during autumn-winter, when irradiance conditions were unfavourable for phytoplankton growth, and Chl *a* showed minimum levels (Fig. 2, 3c and 5e). Furthermore, these authors also showed how seasonal intensification of primary production promoted biogenic settling particles during spring-summer seasons, clarifying why diatom assemblages´ dominant species recorded in the trap material were the same as in the water column (Fig. 4 and 7). With this in mind, our results confirm the major influence of both hydrodynamic and biogenic processes over the diatoms abundance, assemblage composition and export in this coastal upwelling system. The implications of these aspects over the use of diatoms as a proxy of paleoproductivity are discussed hereafter.

5.1. Sediment trap diatom assemblage as a tracer for allocthonous sources in sinking material

Maximum fluxes of benthic diatoms, whose natural habitat is the sediment interface, run parallel with higher wave heights during highly hydrodynamic downwelling periods (Fig. 2c and 6a). This finding along with the fact that during these high-energy episodes lithogenic particle fluxes achieved their maximum levels (as shown in Zúñiga et al., 2016) confirms that strong storms resuspended surface sediments covering the Iberian continental shelf (Dias et al., 2002; Vitorino et al., 2002. Jounneau et al., 2002, Oberle et al., 2014). Furthermore, stormy conditions were accompanied by intense Minho and Douro River discharges which had a significant effect over the water column thermohaline structure (Fig. 2c and 2d). The significant increase in freshwater diatoms associated to river runoff also confirms continental inputs as an additional source of terrestrial material to the inner continental shelf (Fig. 2d and 6c). Indeed, canonical analysis of sediment trap samples revealed a high correlation between benthic and freshwater diatoms, corroborating the co-ocurrence of both resuspension processes and river discharges during downwelling periods (Fig. 8 and Table 2).

One additional evidence of resuspension resulted from the analysis of marine diatom assemblage collected in the sediment trap. *Paralia sulcata* was sporadically found in the water column diatom assemblage during the 2009-2012 studied years (Fig. 4c and Table 3). This meroplanktonic and shadow species, was by contrast, common in ediments and contributed significantly to the trap diatom fluxes during downwelling phases (Fig. 7c and Table 3). As pointed out by previously published sediment trap data from the adjacent Ría de Vigo, this species can be easily resuspended from the sediments under highly hydrodynamic conditions (Bernárdez et al., 2010; Zúñiga et al., 2011). This is, in fact, also supported by the positive relationship found between *Paralia sulcata* and benthic diatoms in the trap samples (Fig. 8 and Table 2).

Also of interest is the positive correlation between freshwater and benthic diatoms to *Thalassiosira eccentrica* (Table 2), a species which is known to occur in areas where nutrient input is continuous throughout the year, such as in areas influenced by river discharge (Moita, 1993, Abrantes and Moita, 1999).

5.2 Seasonal succession of diatom species during upwelling seasons: the imprint of the fossil diatom assemblage

During the studied period, the living diatom community was strongly linked to seasonality revealed by environmental variables, with the highest abundances always recorded during upwelling favourable periods, when irradiance and water column characteristics promote favourable conditions for diatom growth (Fig. 2 and 3).

A detailed analysis of the marine diatom assemblage during upwelling productive seasons revealed that most living species linked to upwelling favourable conditions were either not present (e.g. *Asterionellopsis glaciallis*, *Detonula pumila*, *Guinardia delicatula* and *Skeletonema costatum*) or appeared with a significantly lower contribution in the diatom assemblages (e.g. *Nitzschia* spp., *Pseudo-nitzschia* spp. and small centric) in both sediment trap and the surface sediment sample (Table 3). This observation points to selective dissolution processes acting on thin-walled, less silicified diatoms. As a result, the robust and heavily silicified frustules, not only have a ballast effect that promotes a faster arrival to the sediments, but they also have a higher preservation potential in seafloor sediments (Alexander, 1990; Raven and Waite, 2004). Indeed, diatoms assemblages in both sediment trap and surface sediment samples were mainly composed of highly dissolution resistant *Chaetoceros* and *Leptocylindrus* spp. resting spores (Table 3). This fact confirms that these diatom genera are a good sedimentary indicator of highly productive upwelling conditions. Indeed, the sink of *Chaetoceros* and *Leptocylindrus* spp. resting spores, occurring in close correlation with the dominance of both diatom groups in the water column assemblage during the upwelling periods brings new important information to previous works carried out along the Iberian margin, which have only considered *Chaetoceros* spp. resting spores group as tracer of the coastal upwelling regime (Abrantes, 1988; Bao et al., 1997; Abrantes and Moita, 1999).

Canonical analysis performed for the sediment trap data confirms the relationship between the relative abundances of both *Chaetoceros* and *Leptocylindrus* spp. resting spores with upwelling favourable conditions (positively positioned in CCA1) (Fig. 8). However, they occurred at different times as previously described by other works based on water column data (Figueiras and Rios, 1993; Escaravage et al., 1999; Casas et al., 1999; Nogueira and Figueiras, 2005). The sink of *Chaetoceros* spp. resting spores into the sediment trap was mostly associated to the onset of the upwelling period when irradiance conditions are favourable and persistent northerly winds lead to the upwelling of nutrient-rich subsurface ENACW waters on the shelf. On the contrary, *Leptocylindrus* spp. resting spores fluxes were significantly associated to late-summer autumn when more frequent relaxation of winds promoted water column stratification and nutrient depletion (Fig. 8).

In summary, even though the remobilization of bottom sediments by resuspension processes at the inner NW Iberian continental shelf does not allow for a quantitative evaluation of the water column/sediment record preservation efficiencies, our results bring to light the important role of *Chaetoceros* and *Leptocylindrus* spp. resting spores formation/preservation in determining the primary production paleosignal at this margin. Moreover, the *Chaetoceros* and *Leptocylindrus* spp. spores contribution to the total marine diatom assemblage in sediment records should allow for the identification of persistent vs intermittent upwelling favourable winds in the past, which has important implications for paleoceanographic and paleoclimatic studies.

Acknowledgements

The authors gratefully thank the crew of "R/V *Mytilus*" for their valuable help during the cruises. The authors also want to specially recognize specific lab work made from different members of both the Oceanography group from the Instituto de Investigaciones Marinas de Vigo (CSIC) and the Divisão de Geologia e Georecursos Marinhos from Instituto Português do Mar e da Atmosfera (IPMA). Special thanks to M. Zúñiga for his help in the writing process. This study was sponsored by CAIBEX (CTM2007-66408-C02-01/MAR) and REIMAGE (CTM2011–30155–C03–03) projects funded by the Spanish Government, EXCAPA project (10MDS402013PR) supported by Xunta de Galicia, the EU FEDER funded projects RAIA (INTERREG 2009/2011-0313/RAIA/E) and RAIA.co (INTERREG 2011/2013-052/RAIA.co/1E) and the CALIBERIA project (PTDC/MAR/102045/2008) financed by Fundação para a Ciência e a Tecnologia (FCT-Portugal). D.Z. and E.S. were funded by a postdoctoral fellowship (Plan I2C) from Xunta de Galicia (Spain) and (SFRH/BPD/111433/2015) from FCT, respectively. C.S. was funded by a doctoral grant from FCT (Portugal) (SFRH/BD/88439/2012).

References

Abrantes, F.: Diatoms assemblages as upwelling indicators in surface sediments in Portugal. Mar. Geol. 85, 15-39, 1988.

Abrantes, F., Moita, M.T.: Water column and recent sediment data on diatoms and coccolithophorids, off Portugal, confirm sediment record of upwelling events. Oceanol. Acta, 22(1), 67-84, 1999.

Abrantes, F., Meggers, H., Nave, S., Bollman, J., Palma, S., Sprengel, C., Henderiks, J., Spies, A., Salgueiro, E., Moita, T., Neuer, S.: Fluxes of micro-organisms along a productivity gradient in the Canary Islands region (29ºN): implications for paleoreconstructions. Deep Sea Res. II, 49, 3599-3629, 2002.

Abrantes, F., Gil, I., Lopes, C., Castro, M.: Quantitative diatom analyses: a faster cleaning procedure. Deep Sea Res. II 52, 189-198, 2005.

Abrantes, F., Rodrigues, T., Montanari, B., Santos, C., Witt, L., Lopes, C., Voelker, A.H.L.: Climate of the last millennium at the southern pole of the North Atlantic Oscillation: an inner-shelf sediment record of flooding and upwelling. Clim. Res. 48, 261-280, 2011.

Alexander, RMcN.: Size, speed and buoyancy adaptation in aquatic animals. Am. Zool. 30, 189-196, 1990.

Álvarez-Salgado, X.A., Figueiras, F.G., Pérez, F.F., Groom, S., Nogueira, E., Borges, A.V., Chou, L., Castro, C.G., Moncoiffé, G., Ríos, A.F., Miller, A.E.J., Frankignoulle, M., Savidge, G., Wollast, R.: The Portugal coastal counter current off NW Spain: new insights on its biogeochemical variability. Prog. Oceanogr. 56, 281-321, 2003.

Bakun, A.: Coastal upwelling Indices, West Coast of North America, 1946-71. US Department of Commerce, National Oceanic and Atmospheric Administration, National Marine Fisheries Service, Seattle, WA, 1973.

Bao, R., Varela, M., Prego, R.: Mesoscale distribution patterns of diatoms in surface sediments as tracers of coastal upwelling of the Galician shelf (NW Iberian Peninsula). Mar. Geol. 144, 117-130, 1997.

Battarbee, R. W.: A new method for estimating absolute microfossil numbers with special reference to diatoms. Limnol. Oceanogr. 18, 647-653, 1973.

Bernárdez, P., Prego, R., Varela, M., Francés, G.: Diatom thanatocoenosis in a middle Galician Ría: Spatial patterns and their relationship to the seasonal diatom cycle in the water column and hydrographic conditions. Cont. Shelf Res. 28, 2496-2508, 2008.

Bernárdez, P., Varela, M., Pazos, Y., Prego, R., Francés, G.: Biocenosis and thanatocoenosis of diatoms in a western Galician ría. J. Plank. Res. 32 (6), 857-883, 2010.

Boyd, P.W., and Trull, T.W.: Understanding the export of biogenic particles in oceanic waters: Is there consensus?. Progr. Oceanogr. 72, 276-312, 2007.

Capone, D.G., Hutchins, D.A.: Microbial biogeochemistry of coastal upwelling regimes in a changing ocean. Nature, 6, 711-717, 2013.

Casas, B, Varela, M., Bode, A.: Seasonal succession of phytoplakton species on the coast of A Coruña (Galicia, Northwest Spain). Boletín del Instituto Español de Oceanografía, 15, 413-429, 1999.

Castro, C.G., Nieto-Cid, M., Álvarez-Salgado, X.A., Pérez, F.F.: Local remineralization patterns in the mesopelagic zone of the Eastern North Atlantic, off the NW Iberian Peninsula. Deep Sea Res. I, 53, 1925-1940, 2006.

Dias, J.M.A., González, R., García, C., Díaz-del-Río, V.: Sediment distribution patterns on the Galicia–Minho continental shelf. Prog. Oceanogr. 52 (2–4), 215–231, 2002.

Dormann, C.F., Elith, J., Bacher, S., Buchmann, C., Carl, G., Carré, G., García Marquéz, J.R., Gruber, B., Lafourcade, B., Leitao, P.J., Munkemüller, T., McClean, C., Osborne, P.E., Reineking, B., Schröder, B., Skidmore, A.K., Zurell, D., Lautenbach, S.: Collinearity: a review of methods to deal with it and a simulation study evaluating their performance. Ecography, 36: 27-46, 2013.

Escaravage, V., Prins, T.C., Nijdam, C., Smaal, A.C., Peeters, J.C.H.: Response of phytoplankton communities to nitrogen input reduction in mesocosm experiments. Mar. Ecol. Prog. Series 179, 187-199, 1999.

Espinoza-González, O., Figueiras, F.G., Crespo, B., Teixeira, I.G., Castro, C.G.: Autotrophic and heterotrophic microbial plankton biomass in the NW Iberian upwelling: seasonal assessment of metabolic balance. Aquat. Microb. Ecol. 67, 77-89, 2012.

Falkowski, P.G., Barber, R.T., Smetacek, V.: Biogeochemical controls and feedbacks on ocean primary production. Science, 281, 200, 1998.

Fatela, F., Taborda, R.: Confidence limits of species proportions in microfossil assemblages. Mar. Micropaleontol. 45, 169-174, 2002.

Figueiras, F.G., Pazos, Y.: Microplankton assemblages in three Rías Baixas (Vigo, Arosa and Muros, Spain) with a subsurface chlorophyll maximum: their relationships to hydrography. Mar. Ecol. Prog. Ser. 76, 219-233, 1991.

Figueiras, F.G., Rios, A.F.: Phytoplankton succession, red tides and the hydrographic regime in the Rias Bajas of Galicia. In: Toxic Phytoplankton Blooms in the Sea. T.J., Smayda and Y. Shimizu, Ed. Elsevier Science Publishers B.V., 239-244, 1993.

Figueiras, F.G., Labarta, U., Fernández Reiriz, M.J.: Coastal upwelling, primary production and mussel growth in the Rías Baixas of Galicia. Hydrobiologia, 484, 121-131, 2002.

Fiuza, A.F.G.: Hidrologia e dinâmica das águas costeiras de Portugal. Ph.D. Thesis, Facultade de Ciencias, Univ. Lisboa, Portugal, 1984.

Fraga, F.: Upwelling off the Galician coast, nothwest of Spain. In: Richards, F. (Ed.), Coastal Upwelling. American Geophysical Union, Washington, 176-182, 1981.

Gil, I., Abrantes, F., Hebbeln, D.: Diatoms as upwelling and river discharge indicators along the Portuguese margin: instrumental data linked to proxy information. The Holocene, 17 (8), 1245-1252, 2007.

Hansen, H.P. and Grasshoff, K.: Automated chemical analysis. In: Grasshoff, K., Ehrhadt, M., and Kremling, K. (Eds). Methods of seawater analysis. Verlag Chemie, Weinheim, 347-395, 1983.

Haynes, R., Barton, E.D.: A poleward flow along the Atlantic coast of the Iberian Peninsula. J. Geophys. Res. 95, 11425-11442, 1990.

Jouanneau, J.M., Weber, O., Drago, T., Rodrigues, A., Oliveira, A., Dias, J.M.A., Garcia, S., Schmidt, S., Reyss, J.L.: Recent sedimentation and sedimentary budgets on the wester Iberian shelf. Prog. Ocenogr. 52, 261-275, 2002.

Lange, C.B., Romero, O.E., Wefer, G., Gabric, A.J.: Offshore influence of coastal upwelling off Mauritania, NW Africa, as recorded by diatoms in sediment traps at 2195 m water depth. Deep Sea Res. I, 45, 985-1013, 1998.

LeQuéré, C., Raupach, M., Canadell, J.G., Marland, G. et al.: Trends in the sources and sinks of carbon dioxide. Nature Geoscience, doi: 10.1038/ngeo689, 2009.

Moita, T.: Spatial variability of phytoplankton communities in the upwelling region off Portugal, Proceedings of the International Council for the Exploration of the Sea, L64, 1-20, 1993.

Mortlock, R.A., Froelich, P.N.: A simple method for the rapid determinations of biogenic opal in pelagic marine sediments. Deep Sea Res. 36 (9), 1415–1426, 1989.

Nogueira, E., Figueiras, F.G.: The microplankton succession in the Ría de Vigo revisited: species assemblages and the role of weather-induced, hydrodynamic variability. J. Mar. Sys. 54, 139-155, 2005.

Oberle, F.K.L., Storlazzi, C.D., Hanebuth, T.J.J.: Wave-driven sediment mobilization on a storm-controlled margin. J. Mar. Sys. 139, 362-372, 2014.

Oksanen J., Blanchet F. G., Kindt R., Legendre P., Minchin P. R., O'Hara R. B., et al.: Vegan: Community ecology. Avaliable online at: http://CRAN.R-project.org/package=vegan, 2015.

Onodera, J., Takahashi, K., Honda, M.C.: Pelagic and coastal diatom fluxes and the environmental changes in the northwestern North Pacific during December 1997-May 2000. Deep Sea Res. II, 52, 2218-2239, 2005.

Otero, P., Ruiz-Villarreal, M., Peliz,A., Cabanas, J.M.: Climatology and reconstruction of runoff time series in northwest Iberia: influence in the shelf buoyancy budget off Ría de Vigo. Sci. Mar. 74 (2), 247-266, 2010.

Raven, J.A., Waite, A.M.: The evolution of silicification in diatoms: inescapable sinking and sinking as escape? New Phytol. 162, 45-61, 2004.

Relvas, P., Barton, E.D., Dubert, J., Oliveira, P.B., Peliz, A., da Silva, J.C.B., Santos, A.M.P.: Physical oceanography of the western Iberia ecosystem: Latest views and challenges. Prog. Oceanogr. 47, 149-173, 2007.

Romero, O.E., Lange, C.B., Wefer, G.: Interannual variability (1988-1991) of siliceous phytoplankton fluxes off northwest Africa. J. Plankton Res. 24 (10), 1035-1046, 2002.

Romero, O.E., Armand, L.K.: Marine diatoms as indicators of mordern changes in oceanographic conditions. In: The Diatoms: Applications for the Environmental and Earth Sciences, 2nd Edition, eds. John P. Smol and Eugene F. Stoermer. Published by Cambridge University Press. Cambridge University Press, 373-400, 2010.

Sancetta, C.: Processes controlling the accumulation of diatoms in sediments: a model derived from the british columbian fjords. Paleoceanography, 4 (3), 235-251, 1989.

Sancetta, C.: Diatoms in the Gulf of California: seasonal flux patterns and the sediment record for the last 15 000 years. Paleoceanography, 10(1), 67-84, 1995.

Schrader, H. J., and Gersonde, R.: Diatoms and silicoflagellates. Utrecht Micropaleontol. Bull., 17:129-176, 1978.

Smetacek, V.: Diatoms and the Ocean Carbon Cycle. Protist, 150, 25-32, 1999.

Tenore, K. R., Alonso-Noval, M., Álvarez -Ossorio, M., Atkinson, L.P., Cabanas, J. M., et al.: Fisheries and oceanography off Galicia, NW Spain: Mesoscale spatial and temporal changes in physical processes and resultant patterns of biological productivity. J. Geophys. Res. 100(C6), 10943-10966, 1995.

ter Braak, C. J. F.: Canonical correspondence analysis: a new eigenvector technique for multivariate direct gradient analysis. Ecology, 67, 1167-1179, 1986.

Tréguer, P.J., De La Rocha, C.L.: The world Ocean Silica Cycle. Annu. Rev. Marine Sci. 5, 477-501, 2013.

Utermöhl, H.: Neue Wege in der quantitativen Erfassung des Planktons (mit besonderer Berücksichtigung des Ultraplanktons). Verh. int. Ver. theor. angew. Limnol. 5: 567-596, 1931.

Utermöhl, H.: Zur Vervollkomnung der quantitativen Phytoplankton-Methodik. Mitt. int. Ver. ther. angew. Limnol. 9: 1-38, 1958.

Venrick, E.L., Reid, F.M., Lange, C.B.: Siliceous phytoplankton in the Santa Barbara Channel: a seven-year comparison of species in a near-bottom sediment trap and in water samples from the euphotic layer. CalCOFI Rep., Vol. 44, 2003.

Vitorino, J., Oliveira, A., Jouanneau, J.M., Drago, T.: Winter dynamics on the northern Portuguese shelf. Part 2: bottom boundary layers and sediment dispersal. Progr. Oceanogr. 52 (2–4), 155–170, 2002.

Walsh, J.J.: Importance of continental margins in the marine biogeochemical cycling of carbon and nitrogen. Nature, 350, 53-55, 1991.

Zúñiga, D., Alonso-Perez, F., Castro, C.G., Arbones, B., Figueiras, F.: Seasonal contribution of living phytoplankton carbon to vertical fluxes in a coastal upwellig system (Ría de Vigo, NW Spain). Cont. Shelf Res. 31, 414-424, 2011.

Zúñiga, D., Villacieros-Robineau, N., Salgueiro, E., Alonso-Pérez, F., Rosón, G., Abrantes, F., Castro, C.G.: Particle fluxes in the NW Iberian coastal upwelling system: hydrodynamical and biological control. Cont. Shelf Res. 123, 89-98, 2016.

Table 1. Environmental variables matrix Pearson correlations. Irrad: irradiance; Temp: temperature; Sal: salinity; N^2: Brunt Väisälä frequency parameter; Chl *a*: Chlorophyll *a*; SPM: suspended particulate matter; POC: particulate organic carbon; UI: upwelling index; Minho: Minho River discharge; Waves: Significant wave height in off A Guarda ($WANA_G$) station.

	Irrad	**Temp**	**Sal**	**N^2**	**Chl *a***	**SPM**	**POC**	**NO_3**	**PO_4**	**$Si(OH)_4$**	**Oxygen**	**UI**	**Minho**	**Waves**
Irrad	1.00	-0.394	0.487	-0.0827	0.528	-0.555	0.376	0.0167	0.0764	-0.642	0.148	0.487	-0.236	-0.357
Temp		1.00	-0.263	0.616	-0.196	0.332	0.184	-0.284	-0.195	0.351	-0.346	-0.456	0.0961	0.0557
Sal			1.00	-0.0509	0.228	-0.645	0.348	0.0839	0.263	-0.841	-0.137	0.518	-0.689	-0.27
N^2				1.00	-0.284	0.249	0.124	-0.266	0.0559	0.0825	-0.38	-0.266	-0.101	-0.0122
Chl *a*					1.00	-0.476	0.355	0.0608	-0.0003	-0.321	0.124	0.205	0.0433	-0.272
SPM						1.00	-0.104	0.153	0.0953	0.79	-0.223	-0.409	0.334	0.257
POC							1.00	0.24	0.341	-0.201	-0.39	0.0841	-0.246	-0.242
NO_3								1.00	0.871	0.287	-0.677	0.182	-0.106	-0.252
PO_4									1.00	0.137	-0.823	0.233	-0.274	-0.185
$Si(OH)_4$										1.00	-0.297	-0.466	0.523	0.240
Oxygen											1.00	0.0592	0.213	0.204
UI												1.00	-.0394	-0.116
Minho													1.00	0.139
Waves														1.00

Table 2 Pearson correlation matrix for the sediment trap diatom species relative abundances (%). FW: freshwater diatoms; ChaetoRS: *Chaetoceros* spp. resting spores; Cos.mar: *Coscinodiscus marginatus*; Cos.rad: *Coscinodiscus radiatus*; LeptoRS: *Leptocylindrus* spp. resting spores; Nav: *Navicula* ; Nitzs.mar: *Nitzschia marina*; Par.sulc: *Paralia sulcata*; Pse.Pun: *Pseudo-nitzschia pungens*; Thal.ecc: *Thalassiosira eccentrica*; Thal.nitzs: *Thalassionema nitzschioides*.

	FW	**Benthic**	**ChaetoRS**	**Cos.mar**	**Cos.rad**	**LeptoRS**	**Nav.spp**	**Nitzs.mar**	**Par.sulc**	**Pse.pun**	**Thal.ecc**	**Thal.nitzs**
FW	1.00	0.482	-0.0085	-0.312	0.161	0.226	-0.126	0.176	0.293	0.0318	0.382	-0.0879
Benthic		1.00	-0.38	0.267	0.51	-0.377	0.2	0.0623	0.671	0.159	0.428	0.0777
ChaetoRS			1.00	-0.315	-0.388	-0.0163	-0.147	-0.389	-0.493	-0.318	-0.337	-0.214
Cos.mar				1.00	0.416	-0.137	0.517	-0.138	0.201	0.15	0.182	0.253
Cos.rad					1.00	0.283	0.267	0.0427	0.487	0.0773	0.261	0.202
LeptoRS						1.00	-0.224	-0.107	-0.495	-0.185	-0.0972	-0.173
Nav.spp							1.00	-0.0424	0.196	0.18	0.074	0.174
Nitzs.mar								1.00	0.173	0.547	0.338	0.079
Par.sulc									1.00	0.113	0.288	0.0748
Pse.pun										1.00	0.412	0.561
Thal.ecc											1.00	0.451
Thal.nitzs.												1.00

Table 3. Total abundance and relative contributions of the marine diatom assemblage preserved in the water column, sediment trap and core top sediment sample. SD: Standard deviation. Nitzs: *Nitzschia*; Pseudo-nitzs: *Pseudo-nitzschia*; Thal. nitzs: *Thalassionema nitzschioides*; Nav: *Navicula*. Small centric group in water column samples includes centric diatoms cells which diameter did not allow for species identification and *Thalassiosira* spp. small. Small centric in both sediment trap and surface sediment samples includes: *Coscinodiscus marginatus, Coscinodiscus radiatus*, *Thalassiosira eccentrica*; Chaeto. and Lepto. spp: *Chaetoceros* and *Leptocylindrus* spp. cells and resting spore valves counted in the water column and both sediment trap and surface sediment samples, respectively; Aster. glac: *Asterionellopsis glacialis*; Deton. pum: *Detonula pumila,* Guin. del: *Guinardia delicatula,* Skelet. cost: *Skeletonema costatum.* Most relevant species are highlighted in bold.

	Total	**Nitzs. spp.**	**Pseudo-nitzs. spp.**	**Thal. nitzs.**	**Small centric**	**Nav. spp.**	***Paralia sulcata***	**Chaeto. spp**	**Lepto. spp**	**Aster. glac.**	**Deton. pum.**	**Guin. del.**	**Skelet. cost.**
WATER column													
Upwelling													
cel mL^{-1} (± SD)	717 (1869)	17 (50)	25 (30)	10 (17)	486 (1766)	1 (2)	0 (0)	72 (108)	126 (271)	3 (8)	17 (15)	11 (12)	1 (2)
% (± SD)		3(4)	16 (24)	0.1 (0.4)	20 (31)	0.1 (0.4)	0 (0)	27 (28)	26 (33)	1 (1)	3 (9)	2 (4)	2 (9)
Downwelling													
cel mL^{-1} (± SD)	34 (49)	2 (2)	12 (21)	1 (1)	10 (18)	0 (0)	1 (1)	1 (1)	1 (1)	1 (1)	1 (0)	0 (0)	0 (0)
% (± SD)		12 (12)	18 (28)	2 (4)	52 (25)	2 (4)	2 (4)	7 (10)	1 (3)	2 (3)	2 (7)	0 (0)	0 (0)
TRAP													
Upwelling													
10^4 valves m^{-2} d^{-1} (± SD)	59 (97)	0.2 (0.1)	1.1 (5.8)	0.7 (1.6)	0.5 (0.7)	0.1 (0.3)	5.3 (13)	40.3 (87.2)	23.0 (49.9)	0 (0)	0 (0)	0 (0)	0 (0)
% (± SD)		2 (1)	6 (6)	2 (4)	2 (2)	1 (1)	14 (13)	46 (25)	20 (22)	0 (0)	0 (0)	0 (0)	0 (0)
Downwelling													
10^4 valves m^{-2} d^{-1} (± SD)	216 (462)	0.1 (0.2)	0.1 (0.2)	0.9 (2.1)	1.3 (2.1)	0.3 (0.5)	31.2 (43.6	25.6 (40.6)	43.9 (111)	0 (0)	0 (0)	0 (0)	0 (0)
% (± SD)		1 (1)	1 (1)	2 (2)	3 (2)	1 (1)	23 (12)	28 (19)	24 (19)	0 (0)	0 (0)	0 (0)	0 (0)
SEDIMENT													
GeoB 11002-1													
10^4 valves g^{-1}	142	0	0	2	3	0	24	47	52	0	0	0	0
%		0.2	0	2	2	0	17	33	37	0	0	0	0

Figure captions

Fig. 1. Map of the NW Iberian Peninsula continental margin showing the position of the mooring line (RAIA) site. WANA hindcast reanalysis points 3027034 ($WANA_S$ off Cape Silleiro) and 1044067 ($WANA_G$ off A Guarda) from which wave data were obtained, location of the irrradiance Cíes station (IR) and position of the core-top sediment sample GeoB11002-1 are also shown.

Fig. 2. Temporal series of (a) total irradiance at Cies station (IR), (b) upwelling index ($-Q_x$), (c) significant wave heights (Hs) obtained from the off Silleiro and off A Guarda WANA points and, (d) Minho and Douro River discharges. Upwelling and downwelling periods are highlighted with white and grey bars, respectively, based on upwelling index and biogeochemical data presented in Zúñiga et al. (2016).

Fig. 3. Temporal series of (a) temperature and water column integrated Brunt-Väisälä frequency (N^2), (b) nitrates (NO_3) and silicates ($Si(OH)_4$) content and, (c) diatoms abundance and Chl *a* concentration, measured at 5 m water depth. Upwelling and downwelling periods are highlighted with white and grey bars, respectively, based on upwelling index and biogeochemical data presented in Zúñiga et al. (2016).

Fig. 4. Time series of diatom abundances (a, c, e and g) and assemblages (b, d, f, h) at 5 m water depth. Water column diatom species has been classified in order to easily compare them with fossil diatom assemblage from the sediment trap samples. *Nitzschia* spp: *Nitzschia longissima*; *Pseudo-nitzschia* spp: *Pseudo-nitzschia* cf. *delicatissima* and *Pseudo nitzschia* cf. *seriata*; Thal. nitzs: *Thalassionema nitzschioides*; Small centric: includes centric diatom cells which diameter did not allow for species identification and *Thalassiosira* spp. small; *Navicula* spp: *Navicula transitans* var. *derasa*; *Chaetoceros* (Ch.) spp: Ch. *curvisetus*, Ch. *socialis*, Ch. *didymus*, Ch. *laciniosus*, Ch. *decipiens* and small *Chaetoceros*; *Leptocylindrus* spp: *Leptocylindrus danicus*. Upwelling and downwelling periods are highlighted with white and grey bars, respectively, based on upwelling index and biogeochemical data presented in Zúñiga et al. (2016). The number and the corresponding arrow in figure 4a is referred to small centric cells abundance in July 2010.

Fig. 5. Time series of (a) biogenic silica (BioSi), (c) total siliceous organisms and (e) total diatom (including diatom and spore valves) fluxes registered at RAIA station. Relative contribution of (b) biogenic silica to total mass flux, (d) silicoflagellates respect to total siliceous organisms and (f) resting spores to total diatoms flux are also presented. Upwelling and downwelling periods are highlighted with white and grey bars, respectively, based on upwelling index and biogeochemical data presented in Zúñiga et al. (2016).

Fig. 6. Time series of (a) benthic and (c) freshwater diatom fluxes (and relative contributions respect to total diatoms (b, d)) registered at RAIA station. Upwelling and downwelling periods are highlighted with white and grey bars, respectively, based on upwelling index and biogeochemical data presented in Zúñiga et al. (2016).

Fig. 7. Time series of marine diatoms fluxes (a, c, e) and assemblages (relative contributions to total marine diatoms (b, d, f)) registered at RAIA station. Fossil diatom species has been classified in three groups in order to compare them with water column diatom assemblage. *Nitzschia* spp: *Nitzschia marina*; *Pseudo-nitzschia* spp: *Pseudo-nitzschia pungens*; Thal. Nitzs: *Thalassionema nitzschioides*. Small centric: includes *Coscinodiscus marginatus*, *Coscinodiscus radiatus* and *Thalassiosira*

eccentrica. Upwelling and downwelling periods are highlighted with white and grey bars, respectively, based on upwelling index and biogeochemical data presented in Zúñiga et al. (2016).

Fig. 8. RDA biplot results of the canonical ordination (only significant variables shown) for main fossil sediment trap diatom groups (freshwater (FW) diatoms, benthic diatoms, *Paralia sulcata* (Parsul), *Chaetoceros* spp. spores (ChaeRS) and *Leptocylindrus* spp. spores (LepRS), and forward selected environmental variables (Chlorophyll *a* (Chl *a*), Temperature (Temp), nitrates (NO_3), silicates ($Si(OH)_4$) and Minho River flow). JFM: January-February-March, AMJ: April-May-June, JAS: July-August-September, OND: October-November-December.

Figure 1

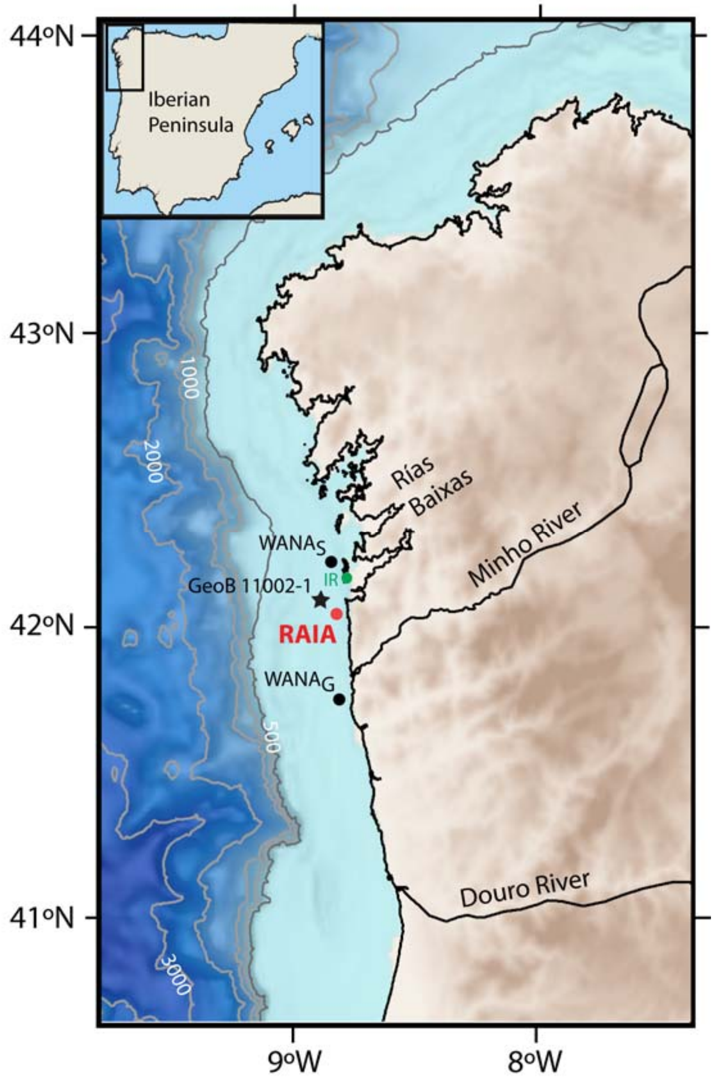
Iberian Peninsula
44ºN
43ºN
42ºN
41ºN
9ºW
8ºW
1000
2000
500
3000
Rías Baixas
Minho River
Douro River
WANA$_S$
IR
GeoB 11002-1
RAIA
WANA$_G$

Figure 2

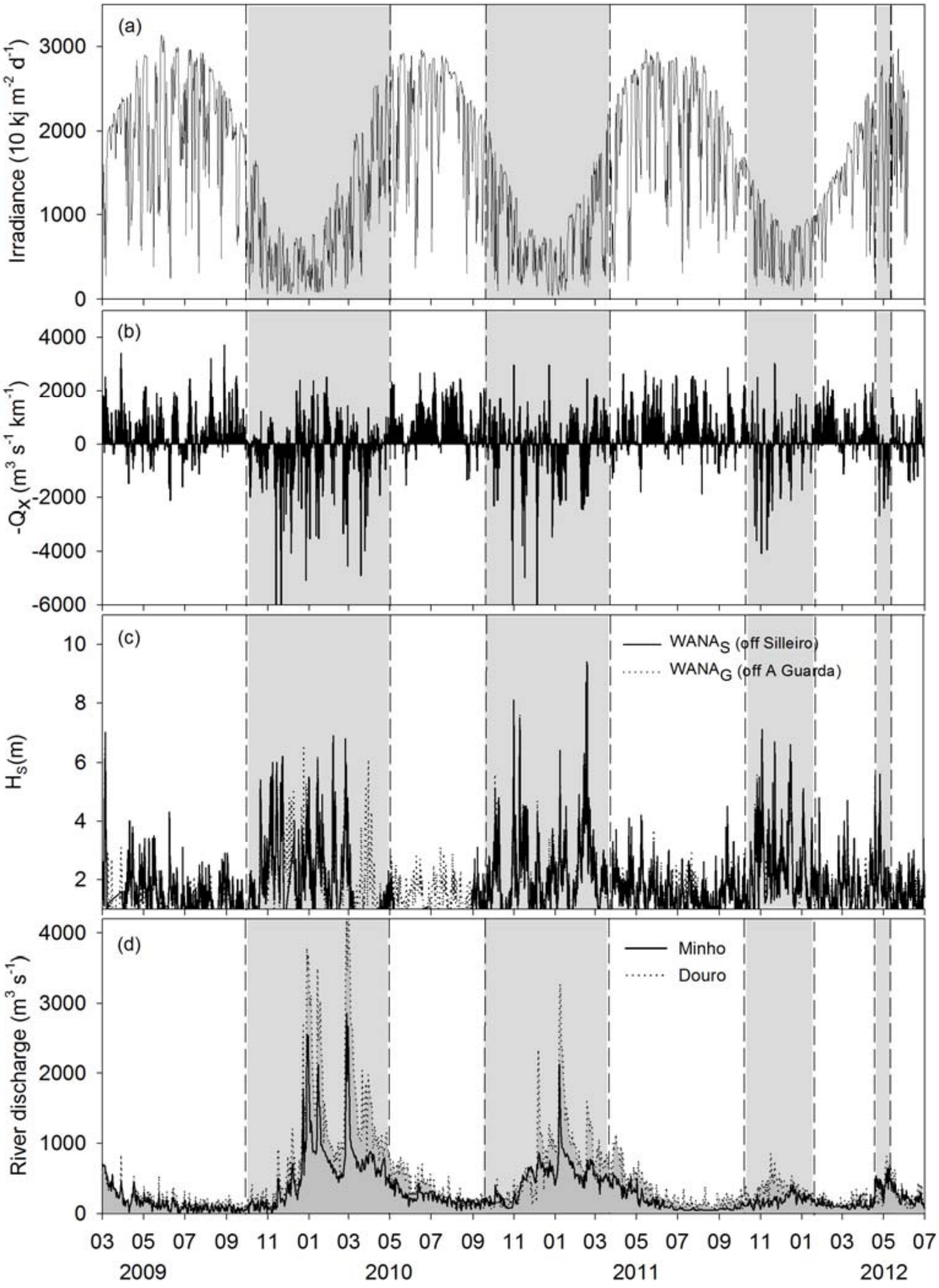
(a)
Irradiance (10 kj m-2 d-1)
3000
2000
1000
0
(b)
-Qx (m3 s-1 km-1)
4000
2000
0
-2000
-4000
-6000
(c)
WANAS (off Silleiro)
WANAG (off A Guarda)
HS(m)
10
8
6
4
2
(d)
Minho
Douro
River discharge (m3 s-1)
4000
3000
2000
1000
0
03 05 07 09 11 01 03 05 07 09 11 01 03 05 07 09 11 01 03 05 07
2009
2010
2011
2012

Figure 3

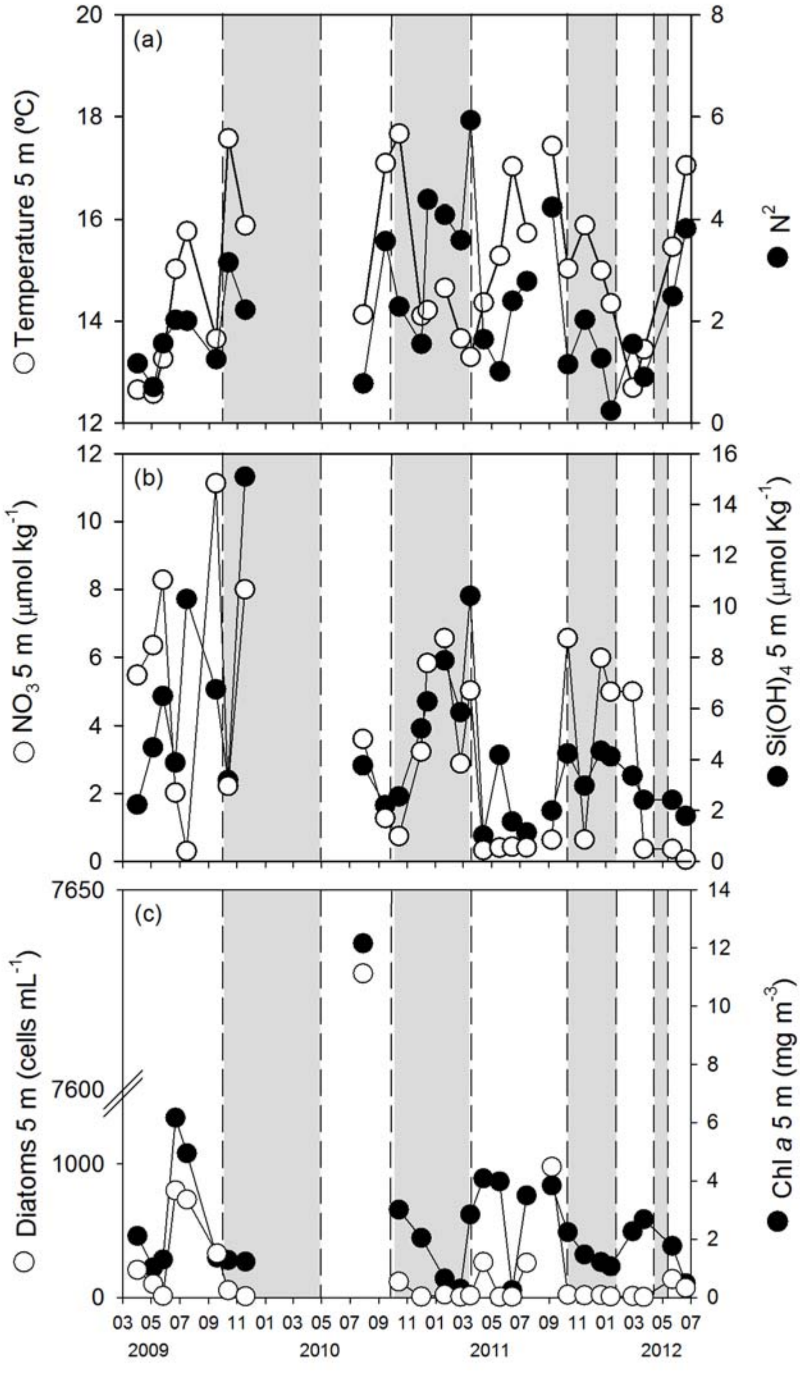
(a)
(b)
(c)
○ Temperature 5 m (ºC)
● N^2
○ NO$_3$ 5 m (µmol kg^{-1})
● Si(OH)$_4$ 5 m (µmol Kg^{-1})
○ Diatoms 5 m (cells mL^{-1})
● Chl *a* 5 m (mg m^{-3})
20
18
16
14
12
8
6
4
2
0
12
10
8
6
4
2
0
16
14
12
10
8
6
4
2
0
7650
7600
1000
0
14
12
10
8
6
4
2
0
03 05 07 09 11 01 03 05 07 09 11 01 03 05 07 09 11 01 03 05 07
2009
2010
2011
2012

Figure 4

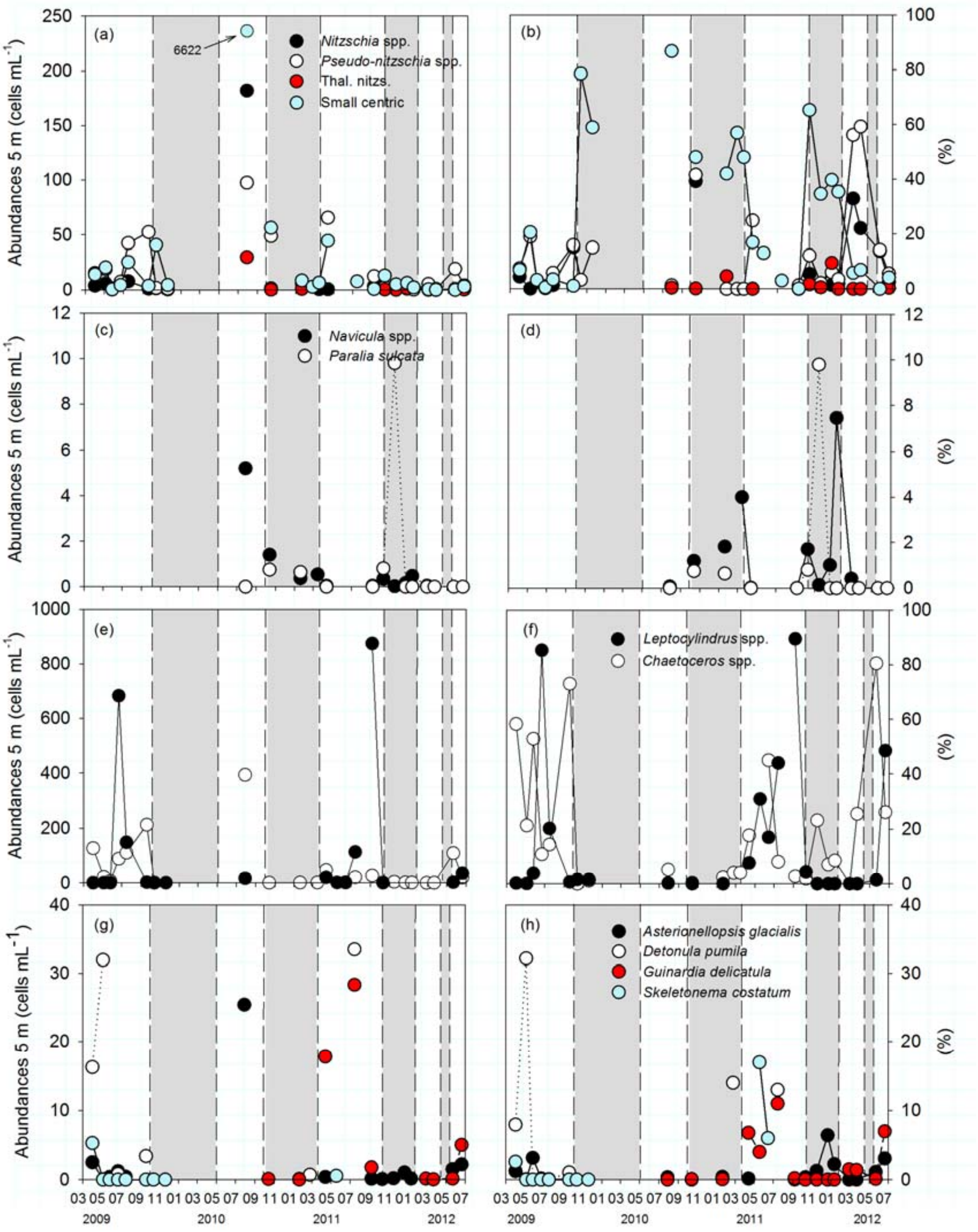
(a)
(b)
(c)
(d)
(e)
(f)
(g)
(h)
6622
Nitzschia spp.
Pseudo-nitzschia spp.
Thal. nitzs.
Small centric
Navicula spp.
Paralia sulcata
Leptocylindrus spp.
Chaetoceros spp.
Asterionellopsis glacialis
Detonula pumila
Guinardia delicatula
Skeletonema costatum
Abundances 5 m (cells mL^{-1})
(%)
0
50
100
150
200
250
0
20
40
60
80
100
0
2
4
6
8
10
12
0
200
400
600
800
1000
0
10
20
30
40
03 05 07 09 11 01 03 05 07 09 11 01 03 05 07 09 11 01 03 05 07
2009
2010
2011
2012

Figure 5

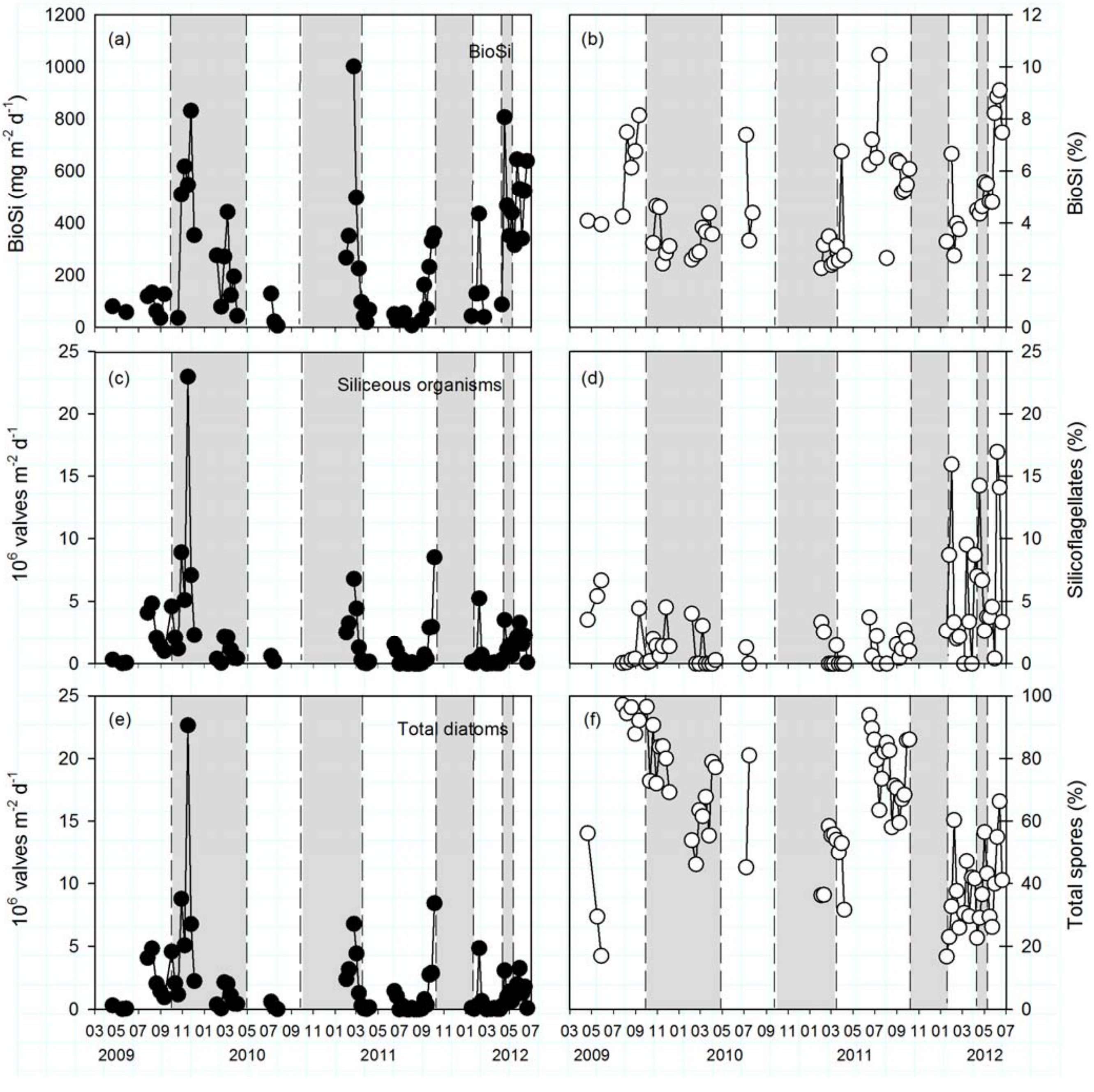
(a)
BioSi
BioSi (mg m^{-2} d^{-1})
0
200
400
600
800
1000
1200
(b)
BioSi (%)
0
2
4
6
8
10
12
(c)
Siliceous organisms
10^6 valves m^{-2} d^{-1}
0
5
10
15
20
25
(d)
Silicoflagellates (%)
(e)
Total diatoms
10^6 valves m^{-2} d^{-1}
(f)
Total spores (%)
0
20
40
60
80
100
03 05 07 09 11 01 03 05 07 09 11 01 03 05 07 09 11 01 03 05 07
2009
2010
2011
2012

5

Figure 6

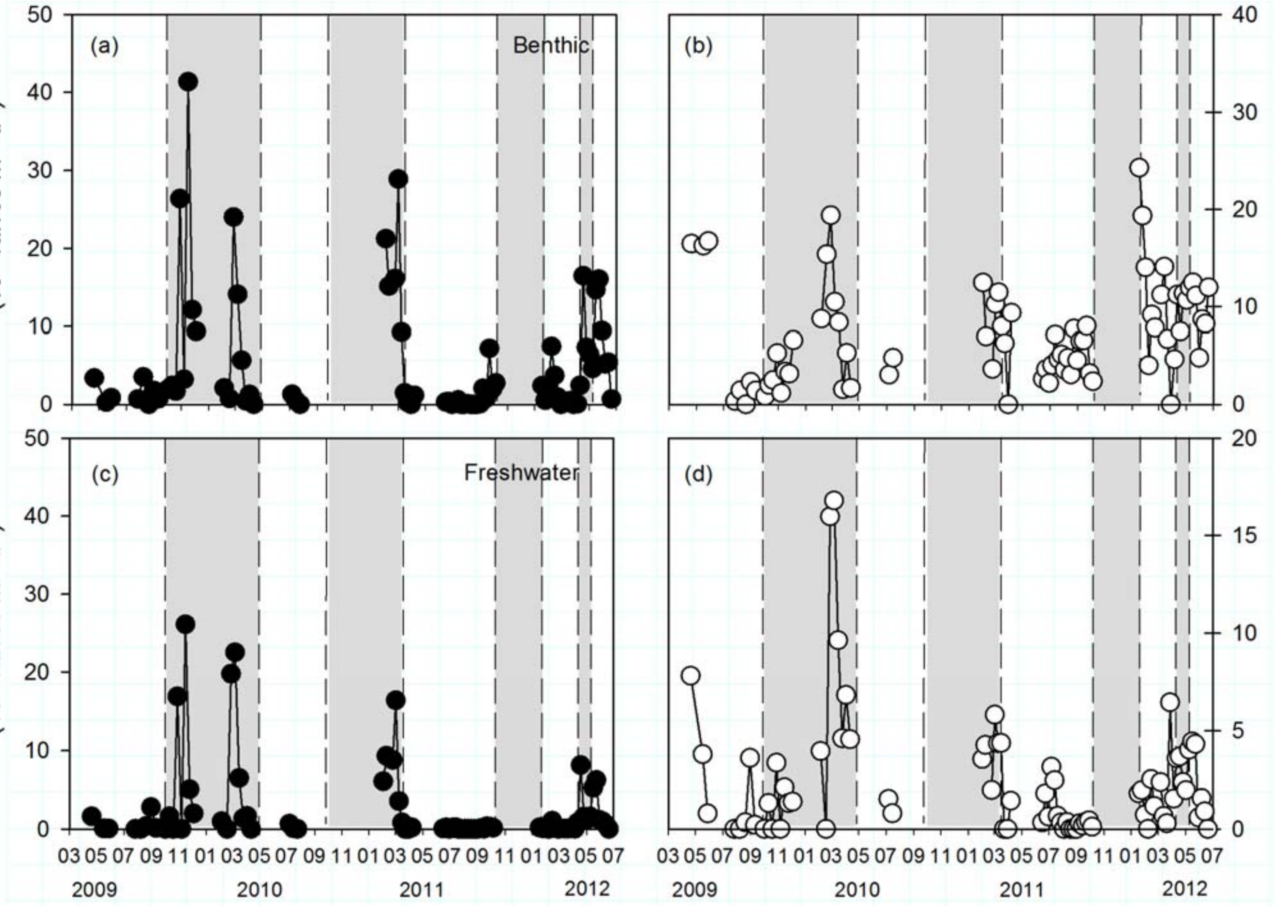
(a)
Benthic
(b)
(c)
Freshwater
(d)
(10^4 valves m^-2 d^-1)
Benthic (%)
Freshwater (%)
0
10
20
30
40
50
03 05 07 09 11 01 03 05 07 09 11 01 03 05 07 09 11 01 03 05 07
2009
2010
2011
2012

5

10

Figure 7

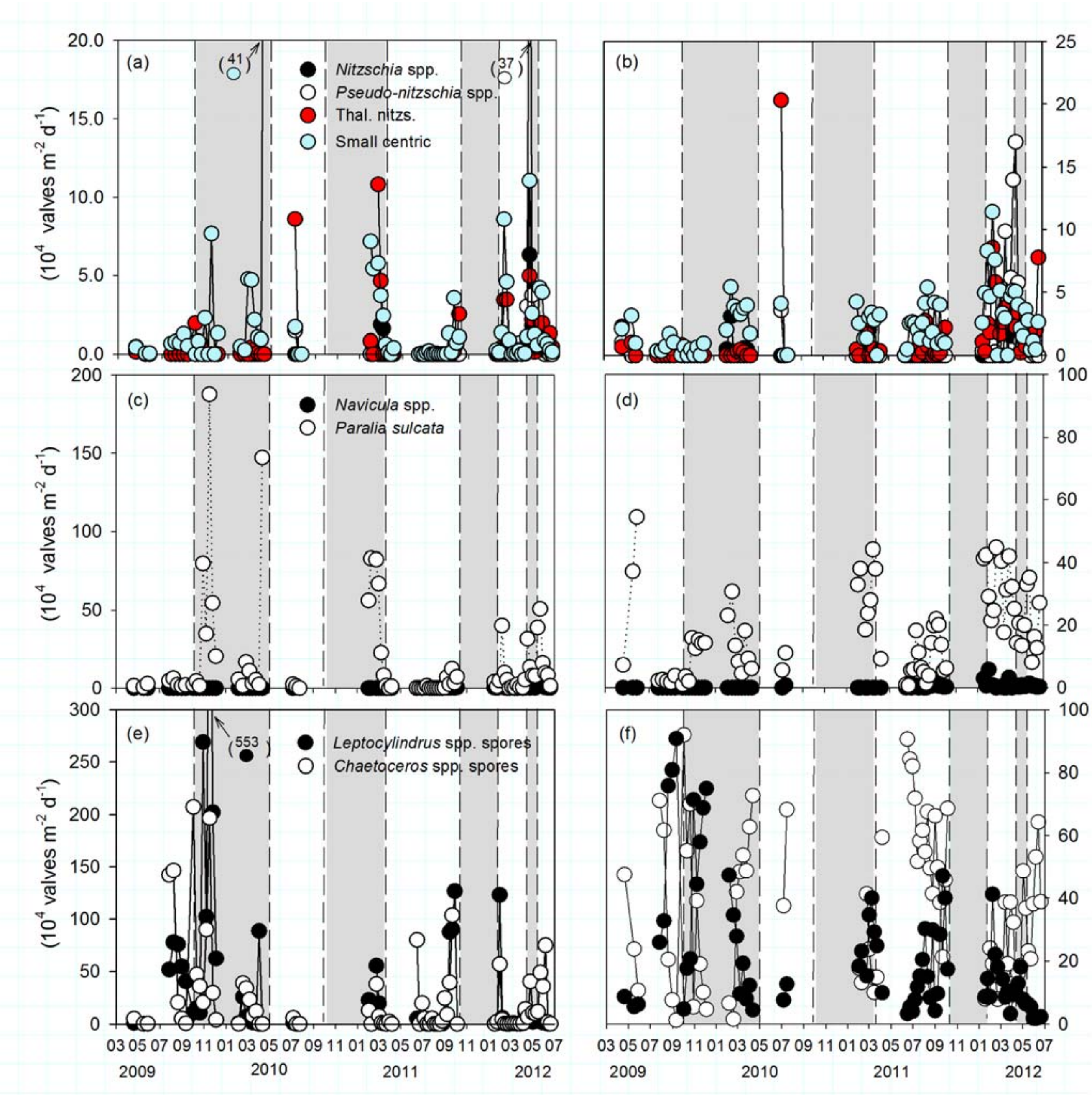

(a)
(b)
(c)
(d)
(e)
(f)
Nitzschia spp.
Pseudo-nitzschia spp.
Thal. nitzs.
Small centric
Navicula spp.
Paralia sulcata
Leptocylindrus spp. spores
Chaetoceros spp. spores
(41)
(37)
(553)
(10^4 valves m^{-2} d^{-1})
(%)
20.0
15.0
10.0
5.0
0.0
200
150
100
50
0
300
250
200
150
100
50
0
25
20
15
10
5
0
100
80
60
40
20
0
03 05 07 09 11 01 03 05 07 09 11 01 03 05 07 09 11 01 03 05 07
2009
2010
2011
2012

5

Figure 8

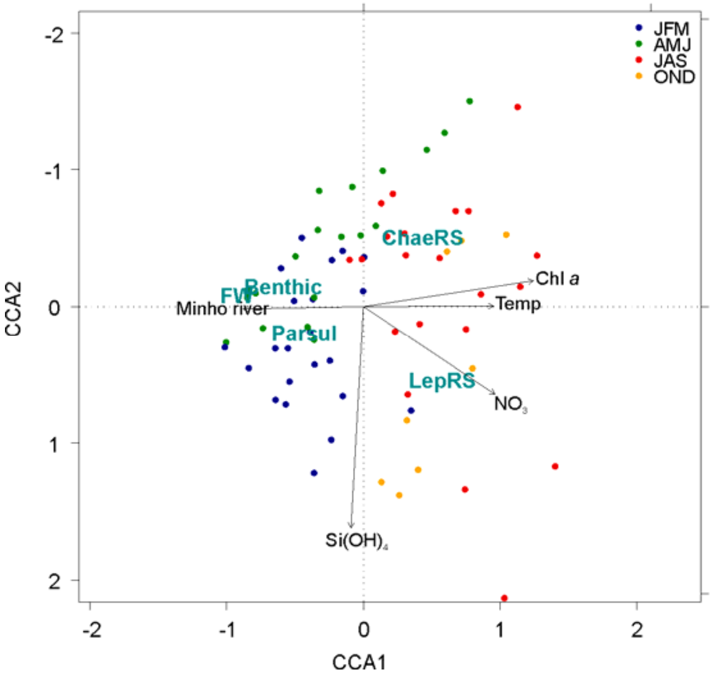
JFM
AMJ
JAS
OND
ChaeRS
Benthic
FW
Minho river
Parsul
LepRS
Chl *a*
Temp
NO_3
$Si(OH)_4$
CCA1
CCA2
-2
-1
0
1
2

Appendix A. List of diatom species found in both the RAIA sediment trap and surficial sediment sample (Geo B 11002). Species that appeared in more than one sediment trap sample with a percentage higher than 2% of the total abundance are highlighted in bold. Ecology preferences: B: benthic; MP: meroplanktonic; P: planktonic; CO: coastal; O: open ocean; C: cosmopolitan; M: marine; MB: marine to brackish; BF: brackish to freshwater; BR: brackish; FW: freshwater.

Diatom species	**Ecology**	**Sediment trap**	**Sediments**
Achnanthes brevipes C. Agardh	B-MB	X	X
Achnanthes sp. (cf. FW)	B-FW	X	
Actinocyclus curvatulus Janisch	P-M-C	X	X
Actinocyclus octonarius Ehrenberg	P-M-C	X	
Actinoptychus senarius (Ehrenberg) Ehrenberg	MP-C	X	X
Actinocyclus sp.	P	X	X
Amphora gracilis Ehrenberg	B-FW	X	
Amphora marina T.V. Desikachary & P. Prema	B-MB	X	
***Amphora* sp.**	B	X	
Anorthoneis excentrica (Donkin) Grunow	B-M	X	
Asteromphalus flabellatus (Brébisson) Greville	P-M	X	
Asteromphalus sp.	P-M-O	X	
Aulacoseira cf. *granulata* (Ehrenberg) Simonsen	P-FW	X	X
Aulacoseira sp.	P-FW	X	X
Azpeitia neocrenulata (S.L.VanLandingham)	P-M	X	
Azpeitia nodulifera (A.Schmidt) G.A.Fryxell & P.A.Sims	P-M	X	
Bacillaria paxillifera (O.F. Müller) T.Marsson	B-P-M	X	
Bacteriastrum hyalinum Lauder	P-M	X	
Caloneis sp.	B-MB	X	
Campylodiscus incertus A.W.F. Schmidt	P-M	X	
Campyloneis grevillei (W.Smith) Grunow & Eulenstein	B-M	X	
Campylosira cymbelliformis Grunow ex Van Heurck	B-MB-CO	X	
Catacombas gaillonii (Bory) D.M.Williams & Round	B-M	X	
Cerataulus smithii Ralfs ex Pritchard	B-MB	X	
Chaetoceros lorenzianus Grunow	P-M-CO	X	
Chaetoceros sp.	P-M-CO	X	
***Chaetoceros* sp.** (resting spores)	M-CO	X	X
Cocconeis disculoides (Hustedt) Stefano & Marino	B-M	X	
Cocconeis guttata Husted & Aleem	B-M	X	
Cocconeis hoffmannii Simonsen	B-M	X	
Cocconeis neodiminuta Krammer	B-FW	X	
Cocconeis placentula Ehrenberg	B-FW	X	X
Cocconeis pseudomarginata Gregory	B-M	X	
Cocconeis scutellum Ehrenberg	B-M	X	X
Cocconeis speciosa Gregory	B-M	X	
Cocconeis stauroneiformis (W.Smith) H. Okuno	B-M	X	

Cocconeis sp.	B	X	
Coscinodiscus gigas Ehrenberg	P-M	X	
Coscinodiscus marginatus Ehrenberg	P-M-OC	X	X
Coscinodiscus cf. *oculus-iridis* (Ehrenberg) Ehrenberg	P-M-OC	X	
Coscinodiscus radiatus Ehrenberg	P-M-OC	X	X
Coscinodiscus sp.	P-M	X	
*Ctenophora pulchell*a (Ralfs ex Kützing)	P-BF	X	
Cyclotella meneghiniana Kützing	P-CO-BF	X	X
Cyclotella plitvicensis Husted	P-FW	X	
Cyclotella stelligera Cleve & Grunow in Van Heurck	P-FW	X	
Cyclotella radiosa (Grunow) Lemmermann	P-FW	X	
Cyclotella sp.	P-(FW)	X	
Cyclostephanos sp.	P	X	
Cymbella affinis Kützing	B-FW	X	X
Cymbela sp.	B	X	
Delphineis minutissima (Husted) Simonsen	P-M-CO	X	X
Delphineis surirella (Ehrenberg) G.W. Andrews	P-M-CO	X	
Detonula pumila (Castracane) Gran	P-M-CO	X	
Dimeregramma minor (Gregory) Ralfs ex Pritchard	B-M	X	
Diploneis cf. *bombus* (Ehrenberg) Ehrenberg	B-MB	X	X
Diploneis didymus (Ehrenberg) Ehrenberg	B-MB-BFW	X	
Diploneis smithii (Brébisson) Cleve	B-MB-BFW	X	
Diploneis cf. *stroemii* Husted	B-M	X	
Diploneis suborbicularis (W.Gregory) Cleve	B-M	X	
Diploneis weissflogii (A.W.F.Schmidt) Cleve	B-M	X	
Diploneis sp.	B	X	
Dytilum sp	P-M-CO	X	
Encyonema sp.	B-FW	X	
Epithemia sp.	B-BFW	X	
Eunotia cf. *pectinalis* (Kützing) Rabenhorst	B-FW	X	
Eunotia praerupta (Grunow)	B-FW	X	
Eunotia sp.	B-FW	X	
Fragilariforma constricta (Ehrenberg) D.M.Williams & Round	B-FW	X	
Fragilaria crotonensis (Kitton) Cleve & Möller	B-BFW	X	
Fragilaria inflata (Heiden) Hustedt	B-FW	X	
Fragilaria investiens (W. Smith) Clever-Euler	B-M	X	
Fragilaria schulzii Brockmann	B-M	X	
Fragilaria sp.	B-C	X	
Fragilariforma virescens (Ralfs) D.M.Williams & Round	B-P-FW	X	
Gomphonema sp.	B	X	X
Gomphonema cf. *acuminatum* (Ehrenberg)	B-BFW	X	
Gomphonema cf. *constrictum* (Ehrenberg)	B-FW	X	
Gomphonema parvulum (Kützing) Kützing	B-FW	X	
Grammatophora angulosa (Ehrenberg)	B-M	X	
Grammatophora marina (Lyngbye) Kützing	B-M	X	X
Grammatophora oceanica (Ehrenberg) Cleve	B-M	X	
Grammatophora sp.	B-M	X	
Grammatophora serpentina (Ehrenberg) Hartley	B-M	X	
Haslea sp.	B-P-M-MB	X	
Hantzschia sp.	B-M-MB	X	

	Hemidiscus cuneiformis Wallich	P-M-O	X	
	Hemiaulus sp.	P-M-CO	X	
	Hyalodiscus scoticus (Kützing) Grunow	P-M-CO	X	
	***Leptocylindrus* sp.** (resting spores)	M-CO	X	X
5	*Licmophora abbreviata* (C.Agardh)	B-M	X	
	Licmophora sp.	B-M	X	
	Luticola mutica (Kützing) D.G.Mann	B-FW	X	
	Martyana martyi (Héribaud-Joseph) Round	B-BR-FW	X	
	Melosira moniliformis (O.F.Müller) C.Agardh	B-M	X	
10	*Melosira varians* C.Agardh	P-FW	X	
	Melosira westii W. Smith	P-M-CO	X	X
	Melosira sp.	B-P-M-BR-FW	X	X
	Navicula bacillum Ehrenberg	B-(P)-M-CO	X	
	Navicula cf. *cancellata* Donkin	B-(P)-M-CO	X	
15	*Navicula cincta* (Ehrenberg) Ralfs	B-FW	X	
	Navicula mutica Kützing	B-FW	X	
	Navicula cf. *pennata* A.Schmidt	B-(P)-M-CO	X	
	***Navicula* sp**.	B-(P)	X	
	Nitzschia angularis W. Smith	P-M-CO	X	
20	*Nitzschia longissima* (Brébisson) Ralfs	P-M	X	
	Nitzschia macilenta W. Gregory	M-CO	X	
	Nitzschia marina Grunow	P-M	X	X
	Nitzschia umbonata (Ehrenberg) H. Lange-Bertalot	M-FW	X	
	Nitzschia sp.	P-M-O	X	X
25	***Odontella aurita*** (Lyngbye) C.Agardh	P-M-CO	X	
	Odontella longicruris (Greville) M.A.Hoban	P-M-CO	X	
	Odontella sp.	P-M	X	
	Opephora marina (W. Gregory) Petit	B-M	X	
	Paralia sulcata (Ehrenberg) Cleve	MP-CO	X	X
30	*Petroneis humeros*a (Brébisson ex W.Smith) Stickle & D.G.Mann	B-M	X	
	Pinnularia borealis Ehrenberg	B-FW	X	
	Pinnularia sp.	B	X	
	Pleurosigma elongatum W. Smith	P-BR	X	
	Pleurosigma normanii Ralfs in Pritchard	P-M	X	
35	*Pleurosigma* sp.	P	X	
	*Pleurosira laev*is (Ehrenberg) Compère	P-BR	X	
	Porosira glacialis (Grunow) Jørgensen	P-BR	X	
	Podosira stelliger (Bailey) Mann	P-M	X	X
	Proboscia alata (Brightwell) Sundström)	P-M	X	
40	*Psammodiscus nitid*us (Gregory) Round & Mann	MP-M-CO	X	
	Pseudo-nitzschia pungens (Grunow ex Cleve) G.R.Hasle	P-M-C	X	
	Pseudo-nitzschia seriata (Cleve) H.Peragallo	P-M	X	
	*Rhaphoneis amphicero*s (Ehrenberg) Ehrenberg	B-M	X	
	Rhabdonema arcuatum (Lyngbye) Kützing	B-M	X	
45	*Rhabdonema minutum* Kützing	B-M	X	
	Rhabdonema sp.	B-M	X	
	Rhizosolenia bergonii Peragallo	P-M-O	X	
	Rhizosolenia hebetata (Bailey) Gran	P-M-O	X	
	Rhizosolenia sp.	P-M-O	X	
50	*Rhoicosphenia abbreviata* (C.Agardh) Lange-Bertalot	B-BR-FW	X	

Rhoicosphenia marina (Kützing) M.Schmidt	B-M-CO	X	
Roperia tesselata (Roper) Grunow ex Pelletan	P-M-O	X	X
Staurosirella pinnata (Ehrenberg) D.M.Williams & Round	MP-FW	X	
Staurosirella sp.		X	
Stellarima stellaris (Roper) G.R.Hasle & P.A.Sims	P-M	X	
Stephanodiscus astrea (Ehrenberg) Grunow	P-C	X	
Stephanodiscus sp.	P-C	X	X
Stephanopyxis turris (Greville) Ralfs in Pritchard	P-M	X	
Surirella sp.	B-M-BR	X	
Synedra sp.		X	
Ulnaria ulna (Nitzsch) Compère	B-FW	X	X
Tabellaria fenestrata (Lyngbye) Kützing	B-FW	X	
*Tabellaria flocculos*a (Roth) Kützing	B-FW	X	
Tabellaria sp.		X	
*Tetracyclus glan*s (Ehrenberg) F.W.Mills	B-FW	X	
Thalassiosira eccentrica (Ehrenberg) Cleve	P-M-O	X	X
Thalassiosira cf. leptopus (Grunow) Hasle & G.Fryxell	P-M-O	X	X
Thalassiosira lineata Jousé	P-M-O	X	
*Thalassiosir*a sp.	P	X	X
Thalassionema nitzschioides (Grunow) Mereschkowsky	P-M	X	X
Toxarium undulatum Bailey	P-M	X	
Trachyneis aspera (Ehrenberg) Cleve 1894	B-M-BR	X	X
Triceratium favus Ehrenberg	P-M	X	
Tryblionella angustata W.Smith	P-M	X	
Tryblionella navicularis (Brébisson) Ralfs	B-BR	X	